Photofragmentation, state interaction, and energetics of Rydberg and ion-pair states: Resonance enhanced multiphoton ionization of HI

Helgi Rafn Hróðmarsson, Huasheng Wang, and Ágúst Kvaran

Citation: The Journal of Chemical Physics **140**, 244304 (2014); doi: 10.1063/1.4883900
View online: http://dx.doi.org/10.1063/1.4883900
View Table of Contents: http://scitation.aip.org/content/aip/journal/jcp/140/24?ver=pdfcov
Published by the AIP Publishing

Photofragmentation, state interaction, and energetics of Rydberg and ion-pair states: Resonance enhanced multiphoton ionization of HI

Helgi Rafn Hróðmarsson, Huasheng Wang, and Ágúst Kvaran[a)]
Science Institute, University of Iceland, Dunhagi 3, 107 Reykjavík, Iceland

(Received 9 April 2014; accepted 5 June 2014; published online 24 June 2014)

Mass resolved resonance enhanced multiphoton ionization data for hydrogen iodide (HI), for two-photon resonance excitation to Rydberg and ion-pair states in the 69 600–72 400 cm^{-1} region were recorded and analyzed. Spectral perturbations due to homogeneous and heterogeneous interactions between Rydberg and ion-pair states, showing as deformations in line-positions, line-intensities, and line-widths, were focused on. Parameters relevant to photodissociation processes, state interaction strengths and spectroscopic parameters for deperturbed states were derived. Overall interaction and dynamical schemes to describe the observations are proposed. © *2014 AIP Publishing LLC*. [http://dx.doi.org/10.1063/1.4883900]

I. INTRODUCTION

Spectroscopic and photofragmentation studies of the hydrogen halides have proven to be very valuable to various contemporary fields of photochemistry such as atmospheric chemistry,[1,2] astrochemistry,[3,4] and photochemical synthesis.[5] The UV, VUV, and multiphoton excitation spectroscopy of these compounds is very rich in structure showing clearly resolved rotational bands due to excitation to Rydberg and ion-pair states.[6–11] Spectral perturbations showing as line shifts[7,8,10,12–20] and/or as line intensity fluctuations[7,8,10,12–19,21–23] are frequently observed as effects of state interactions and/or predissociation processes.[7–9,12,13,18,21] These are seen both in absorption[22,24–29] and REMPI spectra.[7,8,10,12–20,23,30–32] Pronounced ion-pair to Rydberg state mixing have been observed experimentally[7–10,12–14,16–20,22,24–26,30,31,33] and predicted theoretically.[21,34] Furthermore, perturbation effects have been shown to be valuable in spectral assignments.[19]

The spectroscopy of the hydrogen halides has proven to highlight clearly the effects of various perturbation terms neglected in the Born-Oppenheimer (BO) approximation, particularly in the cases of interaction between electronically excited Rydberg states ($\Omega = 0, 1, 2, \ldots$) and ion-pair vibrational states ($\Omega = 0$), where both homogeneous ($\Delta\Omega = 0$) and heterogeneous ($\Delta\Omega > 0$) couplings are observed. In the rotational part of the Hamiltonian, $\mathbf{H^{rot}}$, there are three terms that are neglected in the BO approximation, which are responsible for perturbations between different electronic states. These terms are the following:

(i) $(1/2\mu R^2)(\mathbf{L}^+\mathbf{S}^- + \mathbf{L}^-\mathbf{S}^+)$, which causes spin-electronic homogeneous ($\Delta\Omega = 0$) perturbations.
(ii) $-(1/2\mu R^2)(\mathbf{J}^+\mathbf{S}^- + \mathbf{J}^-\mathbf{S}^+)$, which is the S-uncoupling operator.
(iii) $-(1/2\mu R^2)(\mathbf{J}^+\mathbf{L}^- + \mathbf{J}^-\mathbf{L}^+)$, which is the L-uncoupling operator.

The last two terms are responsible for the heterogeneous ($\Delta\Omega > 0$) perturbations.

Interpretations of observed perturbation effects have in turn allowed distinctions between various photodissociation and photoionization pathways.[18,20]

A number of papers have been published, which place emphasis on state interactions, energy transfers, and photodissociation processes, in HCl[16,18,30,31,35–40] and HBr.[18–20] Whereas most of the studies of hydrogen iodide (HI) have focused on the spectral assignments and the energetics of the Rydberg and ion-pair states, little emphasis has been placed on spectral perturbations for HI. Apart from statements concerning perturbation observations,[17,25,33] no detailed analyses of the spectral perturbations for HI have been reported. In this paper we will emphasize the perturbation effects, involving both homogenenous and heterogenenous state interactions, between the following Rydberg and ion-pair states:

(i) The $H^1\Sigma^+(v' = 1)$ and the $m^3\Pi_2(v' = 0)$ Rydberg states and the $V^1\Sigma^+(v' = m + 6)$ ion-pair state.
(ii) The $O^1\Sigma^+(v' = 0)$ and $k^3\Pi_1(v' = 1)$ Rydberg states and the $V^1\Sigma^+(v' = m + 7)$ ion-pair state.
(iii) The $I^1\Delta_2(v' = 0)$ Rydberg state and the $V^1\Sigma^+(v' = m + 9)$ ion-pair state.

Ginter *et al.*[25] have reported perturbation observations in the absorption spectra due to transitions to the $V^1\Sigma^+(v' = m + 6, m + 9)$ and $k^3\Pi_1(v' = 1)$ states and Pratt and Ginter[33] mention intensity anomalies in a REMPI spectrum for a resonance excitation to the $I^1\Delta_2(v' = 0)$ state. (Vibrational levels of the V state are labeled as $v' = m + i$, $i = 0, 1, 2, \ldots$ where m is an unknown integer.) Here line-shifts (LS) as well as line-intensity (LI) and line-width (LW) alterations, hereafter referred to as LS-, LI-, and LW-effects, respectively, are considered. Quantitative and qualitative information, relevant to photodissociation processes, state interaction and spectroscopic parameters for HI are derived.

a)Author to whom correspondence should be addressed. Electronic mail: agust@hi.is. Telephone: +354-525-4672, +354-525-4800. Fax: +354-552-8911.

II. EXPERIMENTAL

Mass resolved REMPI data were recorded for a HI molecular beam, created by jet expansion of a pure gas sample through a pulsed nozzle. Ions were directed into a time-of-flight tube and detected by a microchannel plate (MCP) detector, to record the ion yield as a function of mass and laser radiation wavenumber.

The apparatus used is similar to that described in Refs. 16, 18, 30, 32, and 41–43. Therefore, only a brief description is given here. The radiation was focused onto the HI molecular beam (HI gas sample obtained from Matheson Gas Products, Inc.) by a lens with a 20 cm focal length inside an ionization chamber between a repeller and extractor plates. The number of photons per pulse inside the chamber is estimated to be about 10^{14} and the photon density about 10^{16} cm^{-2}. The gas sample was pumped through a 500 μm pulsed nozzle from a typical backing pressure of about 2.0–2.5 bar. The pressure inside the ionization chamber was around 10^{-6} mbar during experiments. The nozzle was kept open for about 200 μs and the laser beam was typically fired 500 μs after the nozzle was opened. Ions were extracted into a time-of-flight tube and focused on a MCP detector, from which the signals were fed into a LeCroy WaveSurfer 44MXs-A, 400 MHz storage oscilloscope and stored as a function of ion times-of-flight and laser radiation wavenumber. Average signals were evaluated and recorded for a fixed number of laser pulses. The data were corrected for laser power and mass calibrated to obtain ion yield as a function of mass and excitation wavenumber. REMPI spectra for certain ions as a function of excitation wavenumber were obtained by integrating mass signal intensities for the particular ion. Care was taken to prevent saturation effects as well as power broadening by minimizing laser power. Laser calibration was based on observed (2 + 1) iodine atom REMPI peaks.[44] The absolute accuracy of the calibration was typically found to be about ± 2.0 cm^{-1} on the two-photon wavenumber scale.

III. RESULTS AND ANALYSIS

Mass resolved (2 + n) REMPI spectra of HI were recorded for the two-photon resonance excitation region 69 600–72 400 cm^{-1}. Figs. 1(a)–1(c) show spectra for the

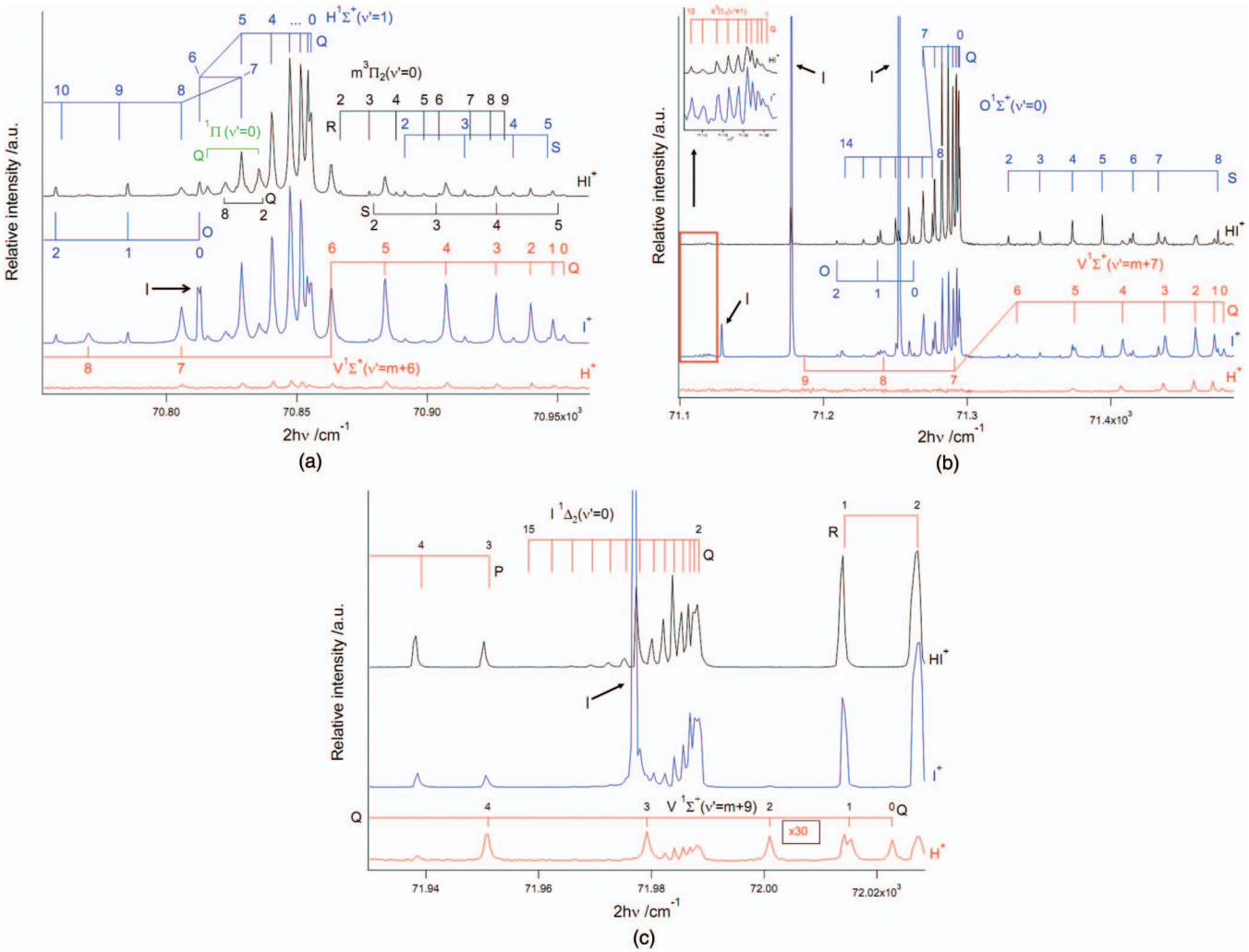

FIG. 1. REMPI spectra for H^+, I^+, and HI^+ and J' assignments of rotational peaks corresponding to two-photon resonance excitation from the ground state to $H^1\Sigma^+(v'=1)$ (a), $V^1\Sigma^+(v'=m+6)$ (a), $m^3\Pi_2(v'=0)$ (a), $O^1\Sigma^+(v'=0)$ (b), $V^1\Sigma^+(v'=m+7)$ (b), $I^1\Delta_2(v'=0)$ (c), $V^1\Sigma^+(v'=m+9)$ (c). (2 + 1) REMPI iodine atomic lines are also marked.[44] The H^+ spectrum in (c) is intensified (×30).

excitation regions 70 710–70 960 cm^{-1}, 71 100–71 490 cm^{-1}, and 71 930–72 030 cm^{-1}, respectively. Peaks due to the two-photon resonance transitions from the ground state $X^1\Sigma^+$ to $H^1\Sigma^+(v'=1)$, $m^3\Pi_2(v'=0)$, $V^1\Sigma^+(v'=m+6)$ (a), $k^3\Pi_1(v'=1)$, $O^1\Sigma^+(v'=0)$, $V^1\Sigma^+(v'=m+7)$ (b), $I^1\Delta_2(v'=0)$, and $V^1\Sigma^+(v'=m+9)$ (c) (hereafter named $H(1)$, $m(0)$, $V(m+6)$, $k(1)$, $O(0)$, $V(m+7)$, $I(0)$, and $V(m+9)$, respectively) are assigned.[17,25] It should be noted that the original assignment of the $H(1)$ state by Ginter *et al.*[25,33] to the $E^1\Sigma^+(v'=0)$ state was reassigned recently.[17] All the major types of spectral perturbations (line-shift (LS), line-intensity (LI), and line-width (LW)-effects) are observed in the spectra. In particular, severe LS-effects are seen in the Q line series for the $H(1)$ and $O(0)$ spectra, where irregular orders of J' quantum numbers are observed (see 1(a) and 1(b)). Analogous effects have been observed for HCl.[15,16] Less severe but clear LS-effects are seen in the Q line series for the $V(m+6)$ spectrum (Fig. 1(a)) and in the S line series for the $O(0)$ spectrum (Fig. 1(b)). Other spectral perturbations, which will be dealt with in more detail below, are less obvious, but significant.

LS-effects refer to deviation of line positions from regular patterns due to rotational energy level shifts because of excited state interactions. This typically shows as nonlinearity in plots of the energy level spacing ($\Delta E_{J',J'-1} = E(J') - E(J'-1)$) vs. J'.[16,18–20] Regular patterns of rotational line positions are determined by transitions to regularly arranged rotational energy levels according to standard energy expressions for unperturbed states, depending on rotational (B_v) and centrifugal distortion (D_v) constants as well as on J' quantum numbers. As an attempt to evaluate the spectroscopic constants, hence the unperturbed energy levels, as well as state interaction strengths (W), from the observed data, simplified deperturbation calculations were performed. Either interactions between one Rydberg vibrational state (1) and one ion-pair vibrational state ($V(v')$; (2)) closest in energy or between two Rydberg states (1a and 1b) and one ion-pair state (2) were considered. The diagonal matrix elements were expressed by the standard energy expressions for the unperturbed energy levels depending on the spectroscopic parameters (see Table I).[45,46] The off-diagonal matrix elements are the interaction strengths (the W's; Table I). The perturbed energy levels were derived from the observed spectral lines and known energy levels for the ground state. The spectroscopic parameters for the states involved as well as the W's were searched for in the deperturbation procedure. In the cases of homogeneous ($\Delta\Omega = 0$) interactions, the W's were assumed to be independent of J', whereas for heterogeneous ($\Delta\Omega \neq 0$) interactions, $W = W'\,(J'\,(J'+1))^{1/2}$, where W' is a constant.

LI-effects appear as abnormal enhancements or drops in ion signal intensities as a function of the J' quantum number. Frequently, "mirror effects" have been observed in the intensity alterations for HCl and HBr,[18,20] in such a way that the ion signal intensity via resonance excitation to one interacting state decreases whereas the ion signal intensity via excitation to the other interacting state increases. This is associated with different ionization processes for the two interacting states. Therefore, ionization of Rydberg states is dominantly found to produce parent molecular ions, whereas ionization of ion-pair states mainly forms fragment ions.[20,30,31] Therefore, ion signal intensity ratios, such as $I(X^+)/I(HX^+)$ vs. J' (X = Cl, Br), have proven to be very useful measures of the J' dependent Rydberg to ion-pair state interactions.[16,18,20,30,31] Furthermore, constant ratio values, independent of J', for the Rydberg states are found to be indicative of dissociation channels.[16–20,25,30,31,33,35–40] An approximation expression for the ion signal intensity ratio in the case of level-to-level interactions for two states (1 and 2) has been derived.[16,18,20,30] The expression depends on the fractional state mixing (c_1^2/c_2^2), state interaction strength (W_{12}), and J' dependent energy level differences ($\Delta E_{J'}$) for the two states as

$$\frac{I(X^+)}{I(HX^+)} = \alpha\frac{\left[\gamma + c_2^2(1-\gamma)\right]}{\left(1-c_2^2\right)}, \tag{1a}$$

$$c_2^2 = \frac{1}{2} - \frac{\sqrt{(\Delta E_{J'})^2 - 4(W_{12})^2}}{2|\Delta E_{J'}|}; \quad c_1^2 = 1 - c_2^2, \tag{1b}$$

and

$$I(X^+) = \alpha_2 c_2^2 + \beta_1 c_1^2; \qquad I(HX^+) = \alpha_1 c_1^2 + \beta_2 c_2^2;$$
$$\alpha = \alpha_2/\alpha_1; \qquad \gamma = \beta_1/\alpha_2; \qquad \alpha\gamma = \beta_1/\alpha_1,$$

where α_1, β_1, α_2, and β_2 are the ionization rate coefficients. γ and $\alpha\gamma$ are measures of X^+ ion formations via dissociation of the Rydberg state, relative to that of the formations of X^+ via excitation of the ion-pair state (γ) and relative to that of the formation of HX^+ via excitation of the Rydberg state ($\alpha\gamma$). Fits of this expression to ion signal intensity ratios vs. J' have allowed evaluation of fractional state mixing as well as the parameters γ and α.[16,18,20,30]

The LS- and LI-effects are found to measure the same effects, namely, bound-to-bound state interactions. The LI-effects, however, are much more sensitive to weak interactions compared to the LS-effects. Thus, weak interaction of

TABLE I. Hamiltonian matrix elements used to derive interaction strengths (W) and spectroscopic parameters (v^0, B', and D') by diagonalization for two-state interaction (a) and a three-state interaction (b). In (a), **1** is a Rydberg vibrational state and **2** is an ion-pair vibrational state ($V^1\Sigma^+(v')$) (see text). v_1^0 and v_1^0 are the relevant term values (band origins). B'_1 and B'_2 are the rotational constants and D'_1 and D'_2 are the centrifugal distortion constants. W_{12} are the interaction parameters. In (b), **1a** and **1b** are Rydberg vibrational states and **2** is an ion-pair vibrational state ($V^1\Sigma^+(v')$) (see text). v_{1a}^0, v_{1b}^0, and v_2^0 are the relevant term values (band origins). B'_{1a}, B'_{1b}, and B'_2 are the rotational constants and D'_{1a}, D'_{1b}, and D'_2 are the centrifugal distortion constants. $W_{1a,2}$ and $W_{1b,2}$ are the interaction parameters.

(a)

	1	**2**
1	E_1^0	W_{12}
2	W_{12}	E_2^0

(b)

	1a	**1b**	**2**
1a	E_{1a}^0	0	$W_{1a,2}$
1b	0	E_{1b}^0	$W_{1b,2}$
2	$W_{1a,2}$	$W_{1b,2}$	E_2^0

$$E_1^0 = v_1^0 + B'_1 J'(J'+1) - D'_1 J'^2(J'+1)^2$$
$$E_2^0 = v_2^0 + B'_2 J'(J'+1) - D'_2 J'^2(J'+1)^2$$
$$E_{1a}^0 = v_{1a}^0 + B'_{1a} J'(J'+1) - D'_{1a} J'^2(J'+1)^2$$
$$E_{1b}^0 = v_{1b}^0 + B'_{1b} J'(J'+1) - D'_{1b} J'^2(J'+1)^2$$
$$E_2^0 = v_2^0 + B'_2 J'(J'+1) - D'_2 J'^2(J'+1)^2$$

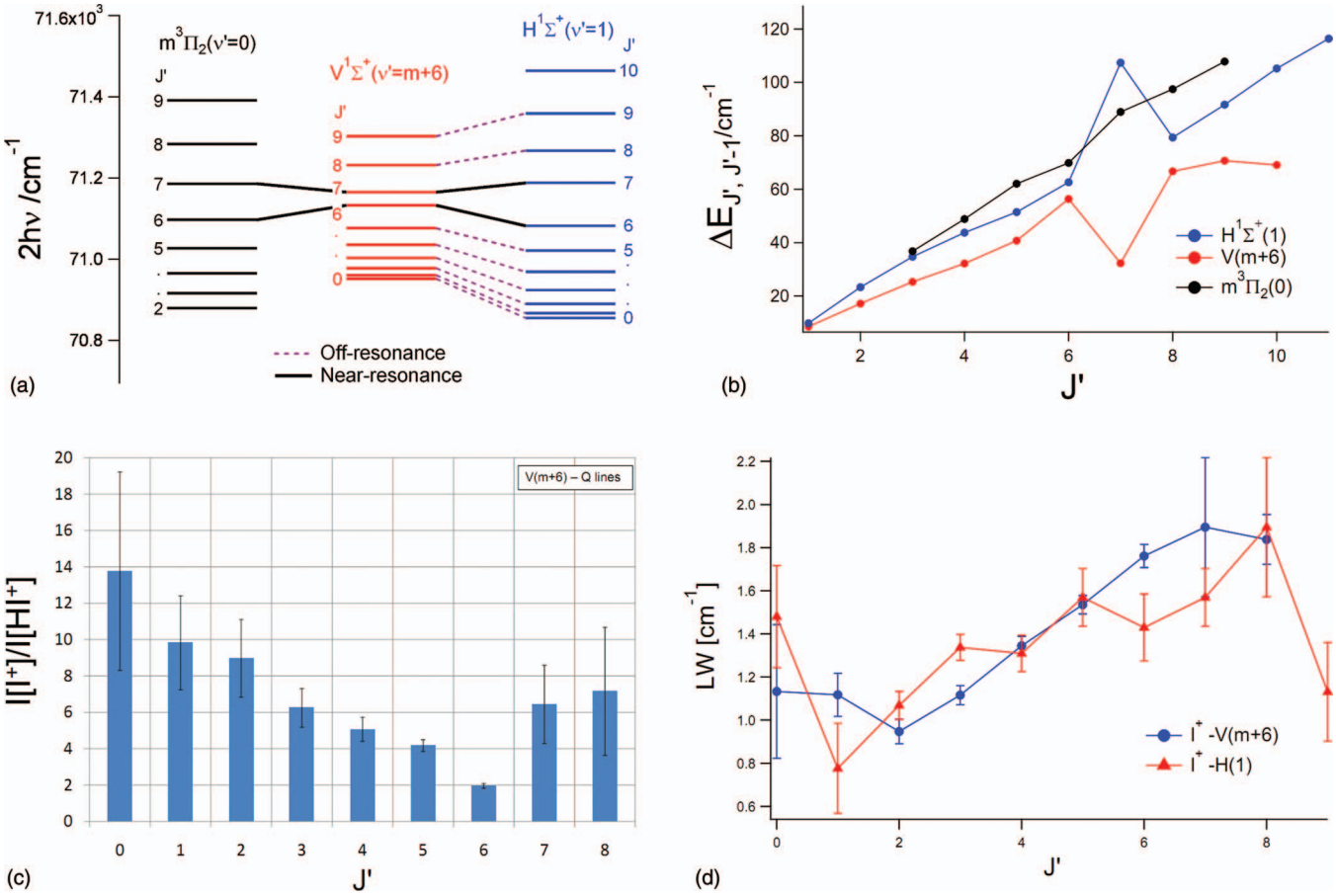

FIG. 2. Figures derived from analysis of REMPI spectra for the $H^1\Sigma^+(v'=1)$, $V^1\Sigma^+(v'=m+6)$, and $m^3\Pi_2(v'=0)$ states (Fig. 1(a)): (a) Rotational energy levels; near- and off-resonance interactions are indicated. (b) Spacing between rotational levels ($\Delta E_{J',J'-1}$) as a function of J'; experimental values. (c) Relative ion-signal intensities ($I(I^+)/I(HI^+)$) vs. J' derived from the Q rotational lines for the $V(m+6)$ state. (d) Rotational line-widths vs. J' derived from the Q lines of the I^+ signals for the $H(1)$ and $V(m+6)$ states.

triplet states and ion-pair states in HCl were found to show clear LI-effects but no significant LS-effects.[30]

The LW-effects appear as J' dependent bandwidths of the ion signals independent of whether it is a parent or a fragment ion. The effects are primarily due to J' dependent lifetimes associated with predissociation processes of Rydberg states.[18,20] These can involve one or more predissociating gateway states in which case the LW-effects also will depend on bound-to-bound state interactions. Thus ion-pair states, which do not predissociate easily, directly,[18–20] can show dramatic LW-effects due to interactions with one or more predissociating Rydberg states in which case the lifetime, hence the line-width, will depend on the Rydberg to ion-pair (bound-to-bound) state interactions as well as predissociation processes of the Rydberg states.[20] Therefore, the rate of dissociation ($1/\tau_2$) of an ion-pair vibrational state (2) has been expressed as a sum of terms, each of which is assumed to be a product of a predissociation rate ($1/t_{1i}$) for a particular Rydberg state (1i) and a J' dependent coupling rate ($f_{1i}(J')$) for the Rydberg to ion-pair state interaction,[20] i.e.,

$$\frac{1}{\tau_2} = \sum_i f_{1i}(J')\frac{1}{\tau_{1i}}. \quad (2)$$

Lower limit lifetimes ($\tau_{\min}$) can be derived from the line-widths (Γ) by[20]

$$\tau_{\min}(\text{ps}) = 5.3/\,\Gamma(\text{cm}^{-1}). \quad (3)$$

A. Off- and near-resonance interactions between the $H^1\Sigma^+(v'=1)$ and $m^3\Pi_2(v'=0)$ Rydberg states and the $V^1\Sigma^+(v'=m+6)$ ion-pair state

The clear LS-effects seen in the spectra of the $H(1)$ Rydberg state and the $V(m+6)$ ion-pair state, mentioned before, where the Q lines for $H(1)$, $J'=6$ and 7 are found to be "clenched" between the corresponding lines for the $V(m+6)$ state (Fig. 1(a)) is indicative of near-resonance interactions. Fig. 2(a) shows the energy levels derived from the rotational lines. Since the $H(1)$ and $V(m+6)$ states share the same symmetry ($^1\Sigma^+$), off-resonance perturbations are also to be expected. Since the band origin (v^0) of the $V(m+6)$ ion-pair state is higher than that for the $H(1)$ state and that the rotational constant for the ion-pair state is smaller, the energy levels of the Rydberg state ($H(1)$) "catch up" with those of the ion-pair state to exhibit the near-resonance interactions for $J'=6$ and 7 (see Fig. 2(a)). The overall interaction

TABLE II. Parameter values, relevant to state mixing, derived from peak intensity-shifts and intensity-ratios ($I(I^+)/I(HI^+)$) as a function of J' (see text), as well as spectroscopic parameters (see Table I) for the state systems $H(1)$, $V(m+6)$, and $m(0)$ (a), $O(0)$ and $V(m+7)$ (b), and $I(0)$ and $V(m+9)$ (c).

(a)

	$H^1\Sigma^+(v'=1)$ Rydberg state/**1a**	$V^1\Sigma^+(v'=m+6)$ ion-pair state/**2**	$m^3\Pi_2(v'=0)$ Rydberg state/**1b**
J'_{res}[a]	6/7	6 /7	6/7
$\lvert\Delta E_{J'}\rvert(cm^{-1})$ for J'_{res}	50.4/23.0	...	35.6/21.0
$W_{1a,2}/\ W_{1b,2}(cm^{-1})$	12.3	...	3.3
$c_1^2\ (c_2^2)$ for J'_{res}	0.93 (0.07)/0.67 (0.33)	...	0.98 (0.02)/0.95 (0.05)
$v^0(cm^{-1})$	70855.5[b]	70952.3[b]	70841.5[b]
	70854.0[c]	70954.0[c]	70840.0[c]
	70850.5[d]	70948.6[d]	70837.6[d]
$B_v(cm^{-1})$	5.77[b]	4.16[b]	6.32[b]
	5.94[c]	3.56[c]	6.21[c]
	6.00[d]	4.09[d]	6.11[d]
$D_v(cm^{-1})$	0.0022[b]	0.0031[b]	0.0025[b]
	−0.0011[c]	0.0024[c]	0.0012[c]
	0.0128[d]	0.0044[d]	0.00019[d]

(b)

	$O^1\Sigma^+(v'=0)$ Rydberg state/1	$V^1\Sigma^+(v'=m+7)$ ion-pair state/2
J'_{res}[a]	7/8	
$\lvert\Delta E_{J'}\rvert(cm^{-1})$ for J'_{res}	32.8/32.8	
$W_{12}(cm^{-1})$	11.0	
$c_1^2\ (c_2^2)$ for J'_{res}	0.86 (0.14)/0.86 (0.14)	
γ	0.93	
α	0.52	
$v^0(cm^{-1})$	71294.7[b]	71478.4[b]
	71290.0[c]	71478.0[c]
	71301.9[e]	
$B_v(cm^{-1})$	6.25[b]	2.95[b]
	6.31[c]	2.96[c]
	5.82[e]	
$D_v(cm^{-1})$	0.0023[b]	−0.0023[b]
	−0.0017[c]	0.0022[c]

(c)

	$I^1\Delta_2(v'=0)$ Rydberg state/1	$V^1\Sigma^+(v'=m+9)$ ion-pair state/2
J'_{res}[a]	2/3	
$\lvert\Delta E_{J'}\rvert(cm^{-1})$ for J'_{res}	12.5/8.5	
$W_{12}(cm^{-1})$	1,1[f]	
	1,3[f]	
$c_1^2\ (c_2^2)$ for J'_{res}	0.99.(0.01)/0.98 (0.02)	
	0.99 (0.01)/0.97 (0.03)	
γ	0.0040	
α	69	
$v^0(cm^{-1})$	71989.4[b]	72023.2[b]
	71990.0[c]	72023.0[c]
	71989.1[e]	72022.4[d]
$B_v(cm^{-1})$	6.31[b]	2.84[b]
	6.306[c]	2.85[c]
	6.312[e]	2.792[c]
$D_v(cm^{-1})$	0.00024[b]	0.0001[b]
	−0.00024[c]	−0.0002[c]
	0.00027[e]	−0.00046[d]

[a] $J'_{res} = J'$ levels closest to resonance interactions (see Figs. 2–4).
[b] Deperturbed values; this work.
[c] Undeperturbed (perturbed) values; this work.
[d] From Ref. 25.
[e] From Ref. 33.
[f] Since the interaction strength, W_{12}, is J' dependent (see text), we present the values obtained from both rotational levels that experience the near-resonance interaction.

effect shows very clearly by the graphs of $\Delta E_{J',J'-1}$ vs. J' for the states involved (see Fig. 2(b)). These show "near-mirror image" effects, such that an increase in $\Delta E_{J',J'-1}$, for one of the states, results in a decrease in the corresponding $\Delta E_{J',J'-1}$ value for the other state and vice versa. This can be explained in the following way with a reference to Fig. 2(a). For the low J's the rotational energies of the $V(m+6)$ ion-pair state are "pushed" upwards and the rotational energies of the $H(1)$ Rydberg state are "pushed" downwards. For $J' = 7$, however, where the energy of the $H(1)$ state exceeds that of the $V(m+6)$ ion-pair state, the Rydberg state experiences a significant increase in energy and the ion-pair state a corresponding lowering in energy resulting in increases and decreases in the corresponding $\Delta E_{7,6}$ values, respectively. For $J' \geq 8$, off-resonance interactions cause the $H(1)$ levels to be "pushed" upwards and the $V(m+6)$ levels to be "pushed" downwards. Energy levels for the $m(0)$ state, derived from the R spectral lines, are shown in Fig. 2(a) and a corresponding $\Delta E_{J',J'-1}$ vs. J' plot is shown in Fig. 2(b). These also show weak but clear effects of near-resonance interactions between the $m(0)$ and the $V(m+6)$ states for $J' = 6$ and 7. Since the total electronic angular moment quantum numbers (Ω) of these states differ by two ($\Delta\Omega = 2$) the interaction must involve a mixing with an $\Omega = 1$ state.[12,23,31] Deperturbation analysis for three states interactions, based on the assignments shown in Fig. 1(a), hence the energy level structure presented in 2(a) and 2(b), gave the rotational constants, B_v, and D_v shown in Table II.

The presence of LI-effects further evidences these state interactions. The largest ion intensity ratios, $(I(I^+)/I(HI^+))$, are observed for the Q lines of the $V(m+6)$ state, showing characteristic lowering in the values as the J's increase from 0 to 6 and an increase for $J' = 7$–8 (Fig. 2(c)). The corresponding ratios for the R lines of the $m(0)$ state are much smaller and constant for $J' = 2$–5 whereas the value for $J' = 7$ is significantly larger.[44] The intensity ratios derived from the Q lines of the $H(1)$ state for $J' = 0$–4 are found to be close to constant. Due to severe peak overlaps in the region of the Q lines for the $H(1)$ state, it is difficult to determine the ion intensity ratios $(I(I^+)/I(HI^+))$ for those J' levels which exhibit near-resonance interactions, quantitatively. Nevertheless, there is a qualitative indication of enhanced ratio values with J' for the $J' = 5$–8 peaks. All in all, these observations are indicative of near-resonance interactions for the $J' = 6$–7 levels and gradually decreasing mixing of the $V(m+6)$ state with Rydberg states as the J' numbers deviate from $J' = 6$ and 7. Furthermore, the constant intensity ratio values, independent of J', for $H(1)$ and $m(0)$ suggests that predissociation of both Rydberg states is important (see above).

Line-widths derived from the Q lines for the $H(1)$ and $V(m+6)$ spectra are shown in Fig. 2(d). Line-widths for the $m(0)$ state (R and S series), were found to be constant,

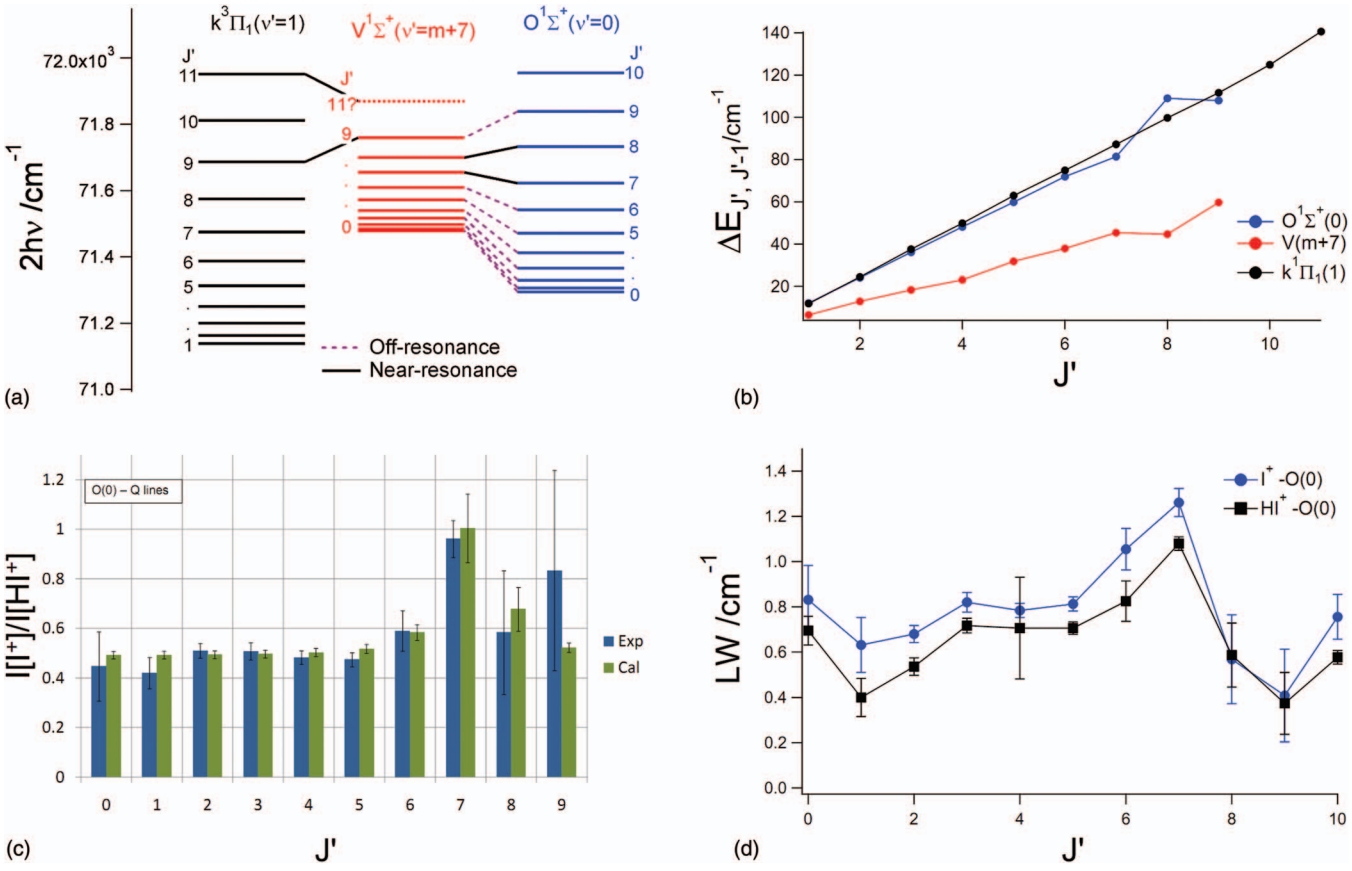

FIG. 3. Figures derived from the analysis of the REMPI spectra for the $k^3\Pi_1(v' = 1)$, $O^1\Sigma^+(v' = 0)$, and $V^1\Sigma^+(v' = m + 7)$ states (Fig. 1(b)). (a) Rotational energy levels. Near- and off-resonance interactions are indicated. (b) Spacing between rotational levels ($\Delta E_{J',J'-1}$) as a function of J'; experimental values. (c) Relative ion-signal intensities $(I(I^+)/I(HI^+))$ vs. J' derived from the Q rotational lines for the $O(0)$ state. (d) Rotational line-widths vs. J' derived from the Q lines of the I^+ and HI^+ signals for the $O(0)$ state.

independent of J', within experimental error, with an average value of about 0.5 cm^{-1}.[44] The line-widths, hence the lifetimes, of the $H(1)$ and $V(m+6)$ states are comparable in terms of the absolute values (0.6–1.9 cm^{-1}) and its J' dependence. By analogy with previous observations for HBr[18] this suggests that the lifetime of the $H(1)$ state is primarily determined by that of the $V(m+6)$ state following its state interaction. Whereas the large average internuclear distance of the V state makes crossing to repulsive states, hence predissociation, highly improbable,[18,20] Rydberg states, on the other hand, are either in close vicinity of, or crossed by, repulsive states to make predissociation processes more probable. Therefore, predissociation of the $V(m+6)$ state is believed to occur via gateway Rydberg states. The predissociating $m(0)$ state is likely to be an important gateway state for the overall $H(1)$ and $V(m+6)$ states predissociation.

B. Off- and near-resonance interactions between the $O^1\Sigma^+(v'=0)$ and $k^3\Pi_1(v'=1)$ Rydberg states and the $V^1\Sigma^+(v'=m+7)$ ion-pair state

In a previous work by Pratt and Ginter,[33] a new Rydberg state was observed at about 71 300 cm^{-1} with the $^1\Sigma^+$ symmetry showing evidence of perturbation effects. This state has been deduced to have a $(\sigma^2\pi^3)4f\pi$ Rydberg orbital and was given the notation $O^1\Sigma^+(v'=0)$. It should be noted that the Rydberg parentage of all of the states mentioned in this paper has been addressed before.[17] It was noted that this Rydberg state was experiencing some perturbation effects due to interactions with the $V(m+7)$ ion-pair state.[17] Here, we will clarify, qualitatively and quantitatively, the nature of this interaction. Furthermore, we will consider evidences for a possible interaction involvement of the $k^3\Pi_1(v'=1)$ state, which is close in energy.

The REMPI spectra of the $O(0)$ and the $k(1)$ Rydberg states as well as the $V(m+7)$ ion-pair state are displayed in Fig. 1(b). The severe LS-effects seen in the spectrum of the $O(0)$ Rydberg state for the Q lines, $J'=7$–8, which are found to be "clenched" between the corresponding Q lines of the $V(m+7)$ state are indicative of near-resonance interactions. Fig. 3(a) shows the energy levels derived from the rotational lines. It shows that a slight enhancement in the energy gap, $\Delta E_{8,7}$, of the $O(0)$ state matches a decrease in the corresponding analogous gap for the $V(m+7)$ state. Slight off-resonance interaction effects are also experienced between levels for different J' values. These effects are clearly seen by the plots of $\Delta E_{J',J'-1}$ vs. J' for the $O(0)$ and $V(m+7)$ states in Fig. 3(b), which exhibit "near-mirror image" effects. Closer inspection of the plots reveals larger enhancement of the $\Delta E_{9,8}$ value for the $V(m+7)$ state compared to that of its corresponding lowering for the $O(0)$ state. This could be due to a near-resonance interaction between the $J'=9$ levels

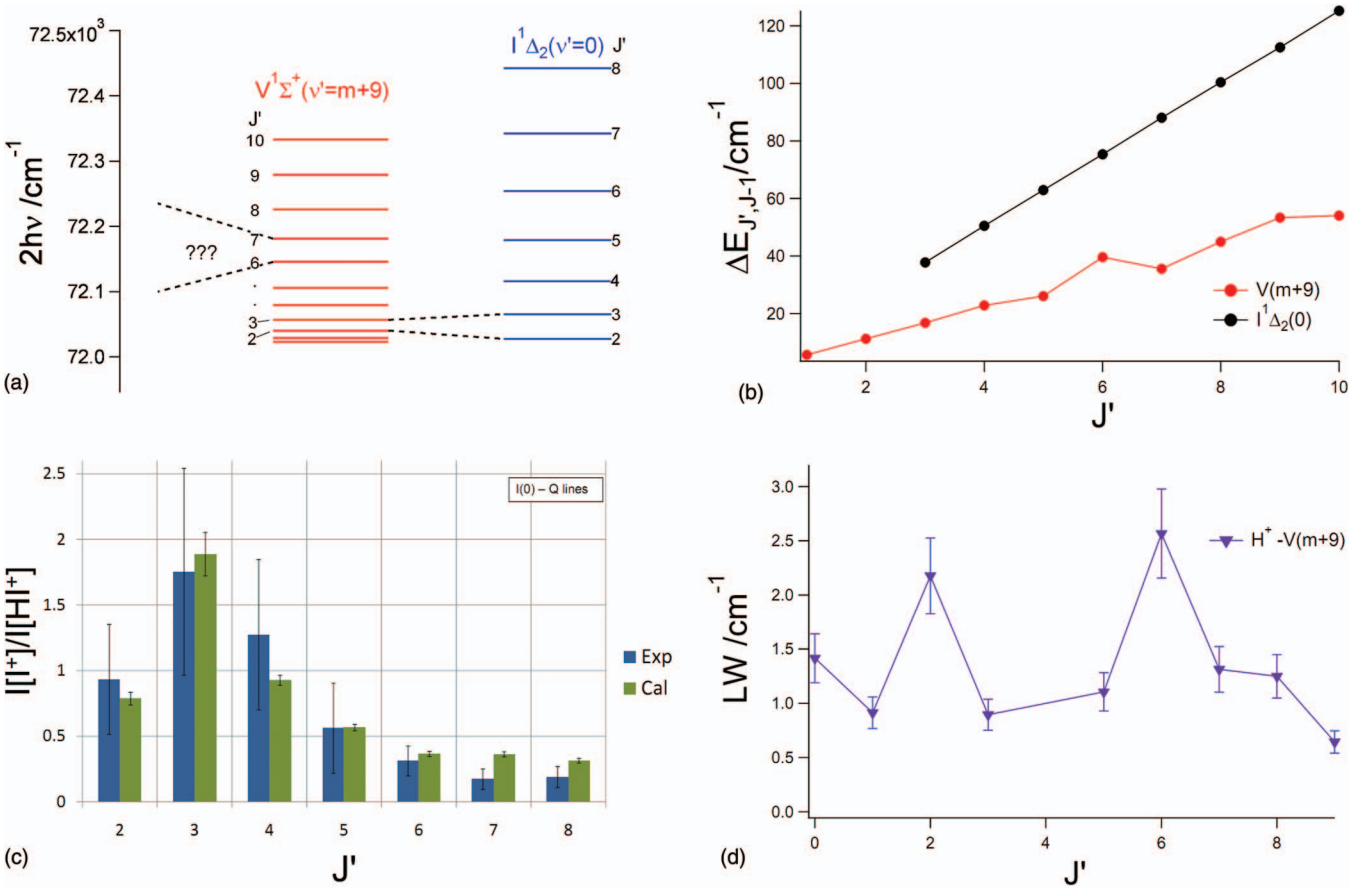

FIG. 4. Figures derived from the analysis of the REMPI spectra for the $I^1\Delta_2(v'=0)$ and $V^1\Sigma^+(v'=m+9)$ states. (a) Rotational energy levels. Near-resonance interactions are indicated. (b) Spacing between rotational levels ($\Delta E_{J',J'-1}$) as a function of J'; experimental values. (c) Relative ion signal intensities ($I(I^+)/I(HI^+)$) vs. J' derived from the Q rotational lines for the $I(0)$ and $V(m+9)$ states. (d) Rotational line-widths vs. J' derived from the Q lines of the H^+ signals for the $V(m+9)$ state.

of the $V(m+7)$ and the $k(1)$ states[17] resulting in still larger energy-gap, $\Delta E_{9,8}$, for the $V(m+7)$ state (see Fig. 3(a)) as well as a lowering in $\Delta E_{9,8}$ for the $k(1)$ state.[17] Furthermore, the drop in $\Delta E_{9,8}$ for the $k(1)$ state is found to be compensated by enhancements in $\Delta E_{10,9}$ and $\Delta E_{11,10}$ for $k(1)$.[17] Due to the lack of observed Q rotational lines for the $V(m+7)$ spectrum for $J' > 9$ the effect of a near-resonance interaction with the $k(1)$ state could not be taken into account in a deperturbation analysis. Deperturbation analysis for two-state interactions, $O(0)$ and $V(m+7)$, based on the assignment shown in Fig. 1(b), hence the energy level structure presented in Figs. 3(a) and 3(b), gave the rotational constants, B_v and D_v, shown in Table II.

The near-resonance interactions between the $O(0)$ and the $V(m+7)$ states are further evidenced by LI-effects. The ion intensity ratios, $I(I^+)/I(HI^+)$, as a function of J' (Fig. 3(c)) for the $O(0)$ state show slight but significant enhancements for $J' = 7$–8. The calculated values, acquired from fitting the data points, are presented in Table II. The relatively large nonzero value derived for γ indicates the importance of a predissociation for the $O(0)$ state, either direct or indirect via gateway Rydberg state(s).

Finally, we consider LW-effects. The line-widths of the Q lines of the $O(0)$ state, derived from the I^+ and HI^+ spectra, are presented in Fig. 3(d). The line-widths for the $k(1)$ state are found to be virtually unchanged with J', within experimental error and comparable in magnitudes to those for the $O(0)$ state.[44] The line-widths of the ion-pair state are found to be larger,[44] hence lifetimes shorter, than those for the Rydberg state. The line-widths of the $O(0)$ system show resemblance to that of the intensity ratios as a function of J' (Fig. 3(c)), both showing a maxima for $J' = 7$. These observations, along with the LI-effects suggest that the predissociation of the $O(0)$ state is partly determined by that of the $V(m+7)$ state[18] following the state interactions as described above. Predissociation of the $V(m+7)$ state will occur via gateway Rydberg states among which the $k(1)$ state is likely to be important.

C. Near-resonance interactions between the $I^1\Delta_2(v' = 0)$ Rydberg state and $V^1\Sigma^+(v' = m+9)$ ion-pair state

REMPI spectra of the $I(0)$ Rydberg state and the $V^1\Sigma^+(m+9)$ ion-pair state show the $J' = 2$ and 3 Q lines of the $I(0)$ state to be "clenched" between the corresponding

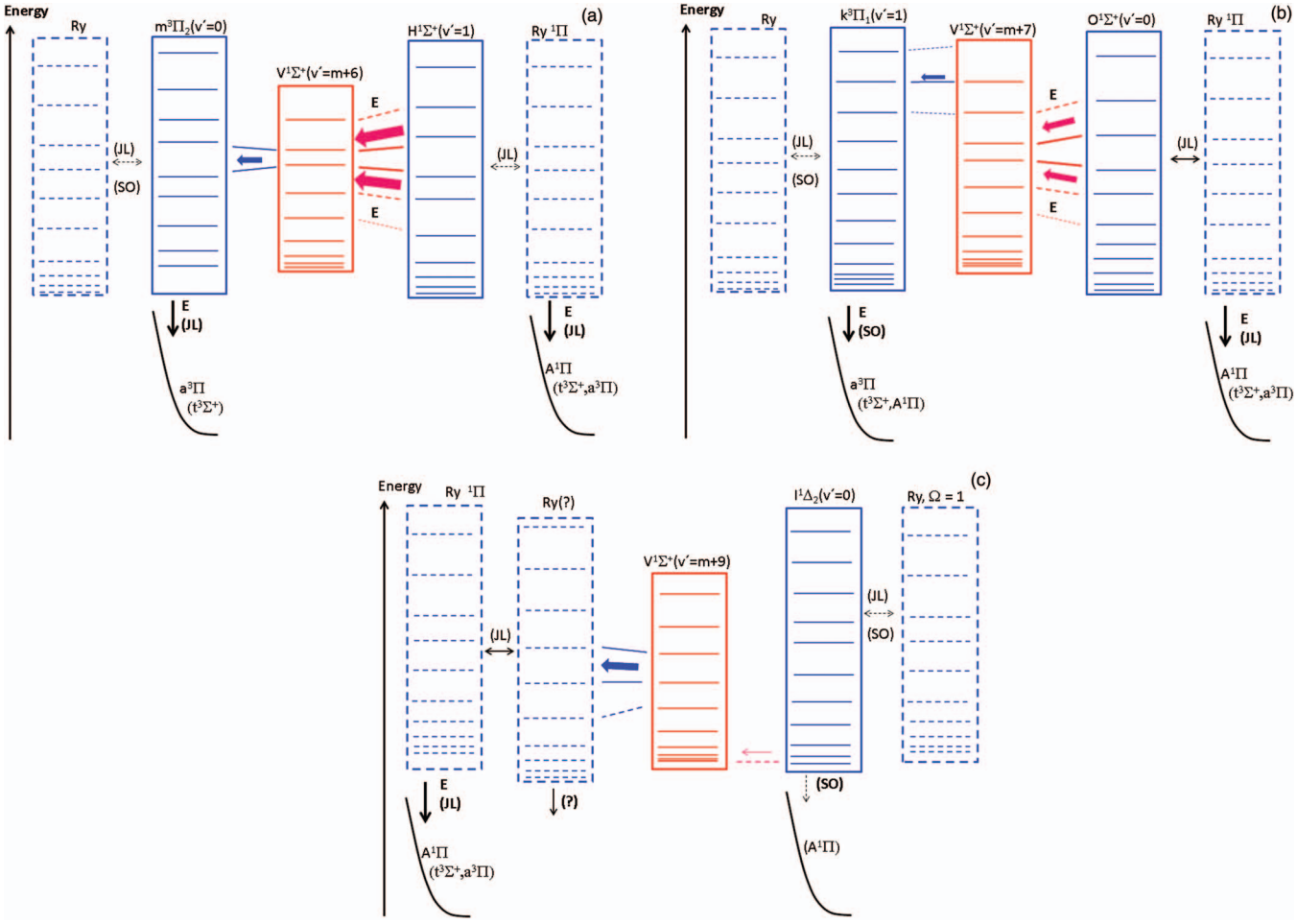

FIG. 5. Semi-schematic figures showing the HI energetics, state interactions, and energy transfers of relevance to the data presented in this paper (see text) for the $H^1\Sigma^+(v' = 1)$, $V^1\Sigma^+(v' = m+6)$, and $m^3\Pi_2(v' = 0)$ states (a), the $O^1\Sigma^+(v' = 0)$, $V^1\Sigma^+(v' = m+7)$, and $k^3\Pi_1(v' = 1)$ states (b) and the $I^1\Delta_2(v' = 0)$ and $V^1\Sigma^+(v' = m+9)$ states (c). Electrostatic, rotational, and spin orbit couplings are marked E, JL, and SO, respectively. Red boxes represent the ion-pair states. Blue boxes are Rydberg states and black curves are repulsive states. The boxes with solid lines represent Rydberg states, which couple with the ion-pair states. The boxes with broken lines are gateway states with respect to predissociation. Relative importance of couplings and transfers is indicated by different boldness of arrows and broken lines as well as by the use of brackets or not. The colored arrows indicate the major paths towards predissociation.

Q lines of the $V(m + 9)$ state.[17] Energy levels derived from the spectra are displayed in Fig. 4(a) and plots of $\Delta E_{J',J'-1}$ vs. J' are shown in Fig. 4(b). Although $\Delta\Omega = 2$ for these states near-resonance interactions might be expected to be found for those levels in the case of a mixing with an $\Omega = 1$ state, by analogy with the observation discussed in Sec. III A. No significant line-shifts due to near-resonance interaction for $J' = 2$–3 are observed, however, whereas an indication of near-resonance interactions with the $V(m + 9)$ state, $J' = 5$–7, is clearly found. Since no Rydberg state with near-resonances for $J' = 5$–7 have been observed,[17,25,33] the corresponding LS-effects must belong to an interaction between the $V(m + 9)$ state and a hidden state. The hidden state could be either a non-observable state due to selection rules for one- and two-photon transitions or a state experiencing weak transition probabilities for transitions from the ground state. Whereas no significant LS-effects are observed for $J' = 2$–3 due to $V(m + 9)$ and $I(0)$ interactions (Fig. 4(a)), LI-effects show as clear ion intensity ratio ($I(I^+)/I(HI^+)$) alternation with J' for $I(0)$ (Fig. 4(c)) indicating weak state interactions. This demonstrates nicely the larger sensitivity of LI-effects compared to that of LS-effects to weak state interactions (see above). Analysis of the intensity ratios, reveal weak interaction strength (W_{12}) and small γ value (see Table II) compared to that derived for the $O(0)$ state (see Sec. III B). The small γ value suggests that predissociation of $I(0)$, either direct or indirect via gateway Rydberg state(s), is of minor importance. Furthermore, there are indications of a slight decrease in the linewidths with J' for $J' \geq 2$ in the case of the $I(0)$ state,[44] suggesting that the lifetime of the $I(0)$ state is primarily determined by these states coupling and by an indirect predissociation of the $V(m + 9)$ state. Furthermore, there are also evidences for enhancements in the linewidths of the H^+ ion signals for the $V(m + 9)$ state as a function of J' for $J' = 2$ as well as for $J' = 6$ (Fig. 4(d)) further indicating the importance of the state interactions in determining the lifetime of the ion-pair state.

IV. SUMMARY AND CONCLUSIONS

Mass resolved REMPI spectra for HI, showing resonance excitation to Rydberg states and ion-pair vibrational states in the two-photon resonance excitation region 69 600–72 400 cm^{-1}, were recorded and analyzed. Three systems of states, all of which have been shown to involve perturbations,[17,25,33] were addressed independently in terms of state interactions. This was done by interpreting observed line-shifts, line-intensity alterations, and line-width effects. In cases when the different observations depend on the same dynamical properties, the analysis results were found to be supportive in nature. Quantitative analysis revealed interaction strengths and spectroscopic parameters for deperturbed states derived from analysis of the line-shifts and parameters (γ and α) relevant to photodissociation processes derived from the line-intensity alterations. Small but significant changes are derived for the spectroscopic parameters, since observed line-shifts are near-resonance in nature, showing as localized shifts of lines and energy levels but limited alterations in overall trends. Nonzero γ values, derived, are measure of the significance of dissociation channels.[16–20,25,30,31,33,35–40] These analyses as well as interpretation of spectral linewidths, hence state lifetimes, allow proposition of state interactions and energy transfers involved in photofragmentation processes for the three energy systems, with reference to Fig. 5,[46,47] as follows:

(i) Fig. 5(a): The $H(1)$ Rydberg state couples mainly with the $V(m + 6)$ state by a strong electrostatic (E) interaction to result in an effective energy transfer from the $H(1)$ state to the $V(m + 6)$ state, followed by further transfer to a manifold of predissociating Rydberg states. Among those is the blended $m(0)$ state, which can predissociate via a strong electrostatic interaction with the repulsive $a^3\Pi$ valence state. Energy flow via direct coupling of the $H(1)$ state with Rydberg states is small.

(ii) Fig. 5(b): The $O(0)$ state couples moderately with the $V(m + 7)$ state by an electrostatic interaction (E) as well as with a Rydberg state close in energy by a rotational coupling (JL). Energy transfer from the $O(0)$ state mainly occurs via the $V(m + 7)$ state to a manifold of predissociating Rydberg states including the $k(1)$ state which predissociates via an electrostatic interaction with the repulsive $a^3\Pi$ state. The direct coupling of the $O(0)$ state with a Rydberg state is likely to involve the $a^1\Pi$ Rydberg state which can couple strongly to the repulsive $A^1\Pi$ state.

(iii) Fig. 5(c): The blended $I(0)$ Rydberg state couples weakly to the $V(m + 9)$ ion-pair state whose lifetime is determined by further coupling to predissociating Rydberg states. A near-resonance interaction between the $V(m + 9)$ state and a hidden Rydberg state is observed.

ACKNOWLEDGMENTS

The financial support of the University Research Fund, University of Iceland and the Icelandic Science Foundation (Grant No. 130259-051) is gratefully acknowledged. We would also like to thank Dr. Jingming Long for useful assistance with the perturbation analysis work.

[1] M. J. Simpson *et al.*, J. Chem. Phys. **130**(19), 194302 (2009).
[2] J. H. Seinfeld and S. N. Pandis, *Atmospheric Chemistry and Physics: From Air Pollution to Climate Change* (John Wiley & Sons, 2006).
[3] J. I. Lunine, *Astrobiology* (Pearson/Addison Wesley, 2005).
[4] A. M. Shaw, *Astrochemistry: From Astronomy to Astrobiology* (Wiley, 2006).
[5] N. Hoffmann, Chem. Rev. **108**(3), 1052 (2008).
[6] A. E. Douglas and F. R. Greening, Can. J. Phys. **57**(10), 1650 (1979).
[7] D. S. Green, G. A. Bickel, and S. C. Wallace, J. Mol. Spectrosc. **150**(2), 303 (1991).
[8] D. S. Green, G. A. Bickel, and S. C. Wallace, J. Mol. Spectrosc. **150**(2), 354 (1991).
[9] D. S. Green, G. A. Bickel, and S. C. Wallace, J. Mol. Spectrosc. **150**(2), 388 (1991).
[10] D. S. Green and S. C. Wallace, J. Chem. Phys. **96**(8), 5857 (1992).
[11] D. Ascenzi *et al.*, Phys. Chem. Chem. Phys. **3**(1), 29 (2001).
[12] Á. Kvaran, H. Wang, and Á. Logadóttir, J. Chem. Phys. **112**(24), 10811 (2000).
[13] Á. Kvaran, Á. Logadóttir, and H. Wang, J. Chem. Phys. **109**(14), 5856 (1998).
[14] Á. Kvaran, H. Wang, and Á. Logadóttir, *Recent Research Developments in Physical Chemistry* (Transworld Research Network, 1998), p. 233.
[15] Á. Kvaran and H. Wang, J. Mol. Spectrosc. **228**(1), 143 (2004).
[16] K. Matthiasson *et al.*, J. Chem. Phys. **134**(16), 164302 (2011).

[17]H. R. Hróðmarsson, H. Wang, and Á. Kvaran, J. Mol. Spectrosc. **290**, 5 (2013).
[18]J. Long, H. Wang, and Á. Kvaran, J. Chem. Phys. **138**(4), 044308 (2013).
[19]J. Long, H. Wang, and Á. Kvaran, J. Mol. Spectrosc. **282** (1), 20 (2012).
[20]J. Long *et al.*, J. Chem. Phys. **136**(21), 214315 (2012).
[21]R. Liyanage, R. J. Gordon, and R. W. Field, J. Chem. Phys. **109**(19), 8374 (1998).
[22]D. S. Ginter, M. L. Ginter, and S. G. Tilford, J. Mol. Spectrosc. **90**(1), 152 (1981).
[23]Y. Xie *et al.*, J. Chem. Phys. **95**(2), 854 (1991).
[24]D. S. Ginter *et al.*, J. Mol. Spectrosc. **92**(1), 55 (1982).
[25]D. S. Ginter, M. L. Ginter, and S. G. Tilford, J. Mol. Spectrosc. **92**(1), 40 (1982).
[26]D. S. Ginter and M. L. Ginter, J. Mol. Spectrosc. **90**(1), 177 (1981).
[27]M. L. Ginter, S. G. Tilford, and A. M. Bass, J. Mol. Spectrosc. **57**(2), 271 (1975).
[28]S. G. Tilford and M. L. Ginter, J. Mol. Spectrosc. **40**(3), 568 (1971).
[29]J. B. Nee, M. Suto, and L. C. Lee, J. Chem. Phys. **85**(2), 719 (1986).
[30]A. Kvaran, K. Matthiasson, and H. S. Wang, J. Chem. Phys. **131**(4), 044324 (2009).
[31]Á. Kvaran *et al.*, J. Chem. Phys. **129**(16), 164313 (2008).
[32]K. Matthíasson, H. Wang, and Á. Kvaran, J. Mol. Spectrosc. **255**(1), 1 (2009).
[33]S. T. Pratt and M. L. Ginter, J. Chem. Phys. **102**(5), 1882 (1995).
[34]M. Bettendorff *et al.*, Zeitschrift Fur Physik a-Hadrons and Nuclei **304**(2), 125 (1982).
[35]A. I. Chichinin, C. Maul, and K. H. Gericke, J. Chem. Phys. **124**(22), 224324 (2006).
[36]A. I. Chichinin, P. S. Shternin, N. Gödecke *et al.*, J. Chem. Phys. **125**(3), 034310 (2006).
[37]S. Kauczok *et al.*, J. Chem. Phys. **133**(2), 024301 (2010).
[38]C. Romanescu *et al.*, J. Chem. Phys. **120**(2), 767 (2004).
[39]C. Romanescu and H.-P. Loock, J. Chem. Phys. **127**(12), 124304 (2007).
[40]C. Romanescu and H.-P. Loock, Phys. Chem. Chem. Phys. **8**(25), 2940 (2006).
[41]Á. Kvaran, K. Matthíasson, and H. Wang, Phys. Chem.: An Ind. J. **1**(1), 11 (2006).
[42]Á. Kvaran, Ó. F. Sigurbjörnsson, and H. Wang, J. Mol. Struct. **790**(1–3), 27 (2006).
[43]A. Kvaran and H. Wang, Mol. Phys. **100**(22), 3513 (2002).
[44]See supplementary material at http://dx.doi.org/10.1063/1.4883900 for iodine atomic lines, intensity ratios, lifetimes, line-shifts, and line-widths.
[45]J. T. Hougen, *NBS Monograph 115* (National Institute of Standards and Technology, Gaithersburg, MD, 1970).
[46]H. Lefebvre-Brion, and R. W. Field, *Perturbations in the Spectra of Diatomic Molecules* (Academic Press, Inc., London, 1986).
[47]M. H. Alexander *et al.*, Chem. Phys. **231**(2–3), 331 (1998).